# Unstable Resonant Orbits near Earth and Their Applications in Planetary Missions

Jeffrey S. Parker*
*Colorado Center for Astrodynamics Research,*
*University of Colorado at Boulder*
*Boulder, CO, 80309*

Martin W. Lo†
*Jet Propulsion Laboratory ,*
*California Institute of Technology,*
*Pasadena, CA, 91109*

**Abstract. This paper explores the uses of planar, simple-periodic symmetrical families of orbits in mission designs in the Earth-Moon system. This classification is defined as the planar periodic orbits that pierce the *x*-axis in the rotating frame exactly twice per orbit where each piercing is orthogonal to the *x*-axis. A continuation method has been used to explore several families of this class of orbit in the Earth-Moon restricted three-body system. The invariant manifolds of the unstable orbits in each of these families are then produced and several mission designs are discussed that take advantage of these manifolds. Focus is given to mission designs that implement resonant orbits that periodically fly by the moon.**

## Nomenclature

| | | |
|---|---|---|
| $C$ | = | Jacobi constant |
| $\mu$ | = | three-body constant, the ratio of the smaller mass to the total mass in the system |
| $\lambda$ | = | eigenvalue |
| $M_1$ | = | primary mass in the three-body system |
| $M_2$ | = | secondary mass in the three-body system ($M_2 < M_1$) |
| $LL_i$ | = | $i^{th}$ Lagrange point in the Earth-Moon system |
| $EL_i$ | = | $i^{th}$ Lagrange point in the Sun-Earth system |

## I. Introduction

THE nature of unstable three-body orbits has only recently been studied with any practical application in mind. Yet, even with incomplete knowledge of the orbital possibilities in the system, many highly successful mission designs have been constructed that have implemented unstable orbits, e.g., the SOHO, WIND, and Genesis missions. The focus of this study is to explore the uses of unstable orbits from the class of planar, simple-periodic symmetrical orbits in the Earth-Moon three-body system. This study will be used as a foundation for further studies of orbits in the Earth-Moon system, including three-dimensional orbits and asymmetric orbits, as part of the development of an architecture to use in missions in the Earth-Moon system.

This study first presents the background for the work in Section I. In Section II it introduces the properties of several families of simple-periodic symmetrical orbits in the Earth-Moon system, including their shapes, stability, and invariant manifolds. Section III discusses orbit transfer options in the system and demonstrates how to take advantage of these invariant manifolds. Finally, Section IV introduces practical applications for these orbit transfers, as well as discussing future extensions for this research.

---

*Doctoral Student, Aerospace Engineering Sciences Department, University of Colorado at Boulder, 431 UCB, Boulder, CO 80309-0431, Student AIAA Member.
†Member of Technical Staff, Navigation and Mission Design Section, Jet Propulsion Laboratory, California Institute of Technology, Pasadena ,CA 91109, AAS Member.

## A. Background

A large amount of work has been completed studying the three-body problem since Newton first formulated it in the late 1600's. It was not until the 1960's that computers were available to numerically search for periodic orbit solutions in the three-body problem. Prior to the 1960's, many simplifications were required in order to begin analytically exploring the system. The planar restricted three-body problem (PCRTBP) was one of the most widely-used models of the three-body problem, especially for motion in the solar system. The general aspects of the periodic orbit solutions in the PCRTBP were well known, primarily because of the work of Strömgren[1], Moulton[2], and Darwin[3], among others. By 1940 no more than a hundred periodic orbits had been computed in the PCRTBP, but the basic properties of several families of orbits had been recognized.

Once computers were available and capable of performing the calculations necessary to integrate orbits in the system, the study flourished as numerical techniques were employed to find new solutions to the problem. By the late 1960's thousands of orbits had been computed, much of the work accomplished by Hénon (Ref. 4-8) among others. A large portion of the solutions to the problem were of the class of simple-periodic symmetrical orbits, as defined by Strömgren.[1] Several satellite missions had begun to be developed that implemented these three-body periodic orbits in their mission designs, including the Genesis mission.

In the recent decade a new method of analyzing dynamical systems has been developed, implementing invariant manifold theory to determine the stable and unstable flows in the system.

## B. Planar Circular Restricted Three-Body Problem

The planar circular restricted three-body problem (PCRTBP) has been used to model the orbits in this study. In general the characteristics of a trajectory modeled in the PCRTBP are preserved when transferring to the full solar system model. Koon et al.[9] demonstrated this when transferring from a libration orbit about the Earth's $L_2$ point to a libration orbit about the Moon's $L_2$ point. Realistically, it is unwise to assume that lunar flybys will be modeled well using the simplifications of the PCRTBP; hence, trajectories that require lunar flybys are avoided in this paper when considering practical mission designs. Nevertheless, the tools that exist that take advantage of the symmetry and simplifications found in the PCRTBP are very helpful in the development of mission designs that would otherwise be very difficult to implement in the full solar system model. Therefore, the PCRTBP has been adopted for this study.

The PCRTBP restricts the movement of all three bodies to the *x-y* plane and assumes the moon is in a circular orbit about the earth. Since the moon's eccentricity and inclination are low, approximately 0.0549 and 5.1454°, respectively,[10] this is a good first-approximation of the dynamics in the system. The coordinate system is set to rotate with the motion of the moon about the earth, where the origin is defined to be at the center of mass of the system. The *x*-axis, also known as the syzygy axis, extends from the origin through the moon, the *z*-axis (which is not used in the model except to set up the axes) extends in the direction of the angular momentum of the system, and the *y*-axis completes the right-hand coordinate frame. It is convenient to normalize the units in the system such that the following metrics are equal to one: the distance between the two primaries, the sum of the two primaries, and the gravitational parameter is set to 1. The three-body constant, $\mu$, is defined as the ratio of the small mass to the large mass, approximately equal to 0.0121506 for the Earth-Moon system. Since the system has been normalized, the coordinates of the earth and moon in the rotating axes are therefore equal to $[-\mu, 0]$ and $[1-\mu, 0]$, respectively. The mass of the third body is neglected in the model.

The equations of motion for the third body in the rotating frame are equal to:

$$\begin{aligned} \ddot{x} &= 2\dot{y} + x - (1-\mu)\frac{x+\mu}{r_1^3} - \mu\frac{x-1+\mu}{r_2^3} \\ \ddot{y} &= -2\dot{x} + y - (1-\mu)\frac{y}{r_1^3} - \mu\frac{y}{r_2^3} \end{aligned} \tag{1}$$

where $r_1$ and $r_2$ are equal to the distance from the third body to the earth and moon, respectively:

$$\begin{aligned} r_1^2 &= (x+\mu)^2 + y^2 \\ r_2^2 &= (x-1+\mu)^2 + y^2 \end{aligned} \tag{2}$$

In this form it is clear that the dynamics of the system depend only on the mass fraction $\mu$. The dynamics of the PCRTBP permit an integral of motion to exist, namely the Jacobi constant, $C$:

$$C = 2U - V^2 \tag{3}$$

where

$$\begin{aligned} U &= \frac{1}{2}\left(x^2 + y^2\right) + \frac{1-\mu}{r_1} + \frac{\mu}{r_2} \\ V^2 &= v_x^2 + v_y^2 \end{aligned} \tag{4}$$

The Jacobi constant is considered only in normalized units; it is nontrivial to convert from the normalized units to SI units.

It is well known that five equilibrium points exist in the PCRTBP, referred to as the Lagrange points. In this study we will adopt the nomenclature that $L_1$ lies between the earth and the moon, $L_2$ beyond the moon, $L_3$ beyond the earth, $L_4$ above the $x$-axis, and $L_5$ below the $x$-axis. Figure 1 shows a plot of the locations of these Lagrange points in the Earth-Moon rotating coordinate system.

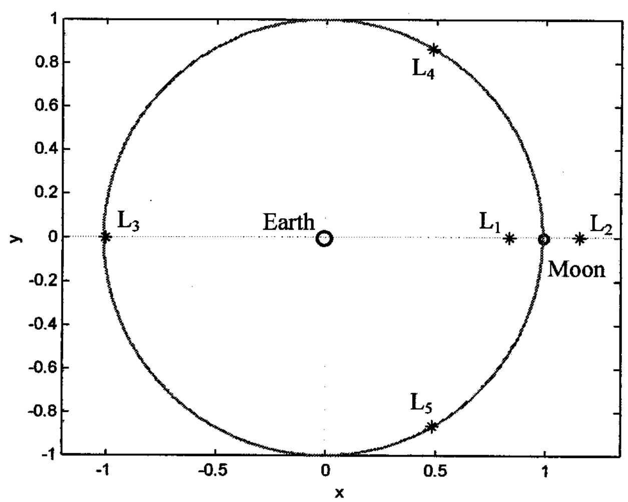


**Figure 1. The earth, moon, and five Lagrange points in the rotating coordinate system of the PCRTBP.**

## C. Finding Symmetric Periodic Orbits in the PCRTBP

A simple differential corrector, given in Ref. 11, has been used in this study to produce symmetric periodic orbits in the PCRTBP. The differential corrector invokes a shooting method to converge on the solutions. The only constraint on the system is that the corrector has been designed to converge on a certain type of solutions, namely orbits that pierce the $x$-axis orthogonally twice per orbit. They may pierce the $x$-axis more times, but must pierce it twice orthogonally. This study has further limited the search to *simple-periodic* orbits,[1] which only pierce the $x$-axis orthogonally. The corrector follows the following procedures:

- The third body begins with initial conditions $(x, y, \dot{x}, \dot{y}) = (x_0, 0, 0, \dot{y}_0)$;
- It is then propagated until it pierces the $x$-axis $n$ times (half of a period);
- For the trajectory to be periodic, the state must now be $(x, y, \dot{x}, \dot{y}) = (x_{T/2}, 0, 0, \dot{y}_{T/2})$, hence all velocity in the $x$-direction is undesirable. The corrector attempts to remove this velocity by adjusting either $x_0$ or $\dot{y}_0$ and keeping the other initial condition constant;

- The process is repeated until a given tolerance is met.

The corrector may be designed to adjust one or the other initial condition of the third body. See Ref. 11 for more information.

### D. The Continuation Method

Periodic orbits in the PCRTBP may be grouped into one-parameter families, where a family contains an infinite number of periodic orbits whose properties vary continuously from one end of the family to the other. This property of the PCRTBP is due to the existence of the Jacobi constant, the PCRTBP's integral of motion.[8] Once a single periodic orbit is known then the continuation method may be used to traverse that orbit's family. One parameter of the known periodic orbit is perturbed and a differential corrector is applied to find that periodic orbit's neighbor in its family. Howell's differential corrector[11] is well-suited to this method for simple-periodic symmetrical orbits because one may vary the initial position and correct for the initial velocity that corresponds to the next periodic orbit in the family (or vice versa, if desired).

To demonstrate this method, the continuation method has been applied to the family of Lyapunov orbits that exist about the Earth-Moon $L_2$ point ($LL_2$). By varying $x_0$, one can produce the plot shown in Figure 2, the initial conditions for those orbits shown in Figure 3. The axes are in the rotating coordinate system, but converted to SI units.

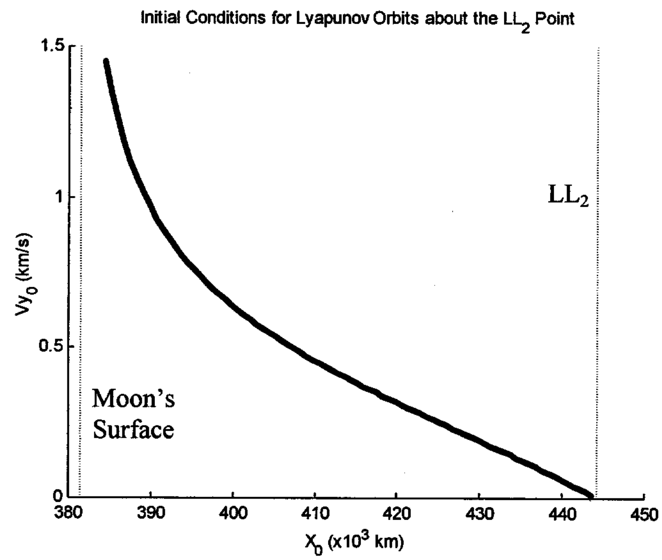


**Figure 2. A plot of the initial conditions of the family of Lyapunov orbits about the Earth-Moon $L_2$ point ($LL_2$).**

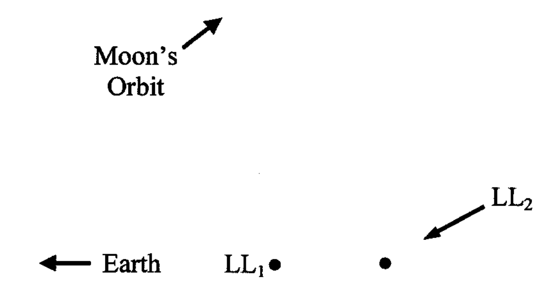


The continuation method works well when the perturbations are small; in practice it is beneficial to predict the differential corrector's adjustment to the perturbation because this allows larger jumps in the varying parameter. Furthermore, if the perturbations are too large, the differential corrector may converge on a solution of a different family. Thus smaller steps or better prediction methods may be required to make the continuation method more reliable. The work for this study implemented a quadratic prediction method that used the three previous data points of the family to predict the next data point. This was sufficient to allow the differential corrector to converge quickly while allowing the curve of the family to evolve naturally over the state space.

### E. Stability

The stability of a periodic orbit can be determined by analyzing the eigenvalues of the orbit's monodromy matrix. Orbits in the PCRTBP have four eigenvalues, $\lambda_i$ for $i = 1,\ldots,4$, corresponding to the eigenvectors $v_i$. The eigenvalues are related in the following way:

$$
\begin{aligned}
\lambda_1 &= \lambda_1, \qquad & \lambda_2 &= \frac{1}{\lambda_1}, \\
\lambda_3 &= \lambda_3, \qquad & \lambda_4 &= \frac{1}{\lambda_3},
\end{aligned} \tag{5}
$$

where the reciprocal of an imaginary eigenvalue is the complex conjugate of that eigenvalue. Periodic orbits in the PCRTBP have at least two imaginary eigenvalues that are complex conjugates of each other. The other two eigenvalues are either imaginary or real numbers. If there is a real eigenvalue outside of the range [-1,1], then the periodic orbit is asymptotically unstable, referred to here as *unstable*, along the corresponding eigenvector. If there are no real eigenvalues outside of that range, then the periodic orbit is *neutrally stable*, or a *center*.[12]

### F. Invariant Manifolds

All periodic orbits have invariant manifolds, but the interesting manifolds for mission design purposes are the stable and unstable invariant manifolds of unstable periodic orbits, referred to as $W^S$ and $W^U$, respectively. An orbit's unstable invariant manifold is composed of the set of all trajectories that a particle could take after a perturbation in the direction of the orbit's unstable eigenvector. In practice any perturbation from the unstable orbit will include at least a small portion of the orbit's dominant unstable eigenvector; that portion will quickly grow and the particle will asymptotically approach the unstable manifold. The orbit's stable manifold is similarly defined as the set of all trajectories that a particle could take to arrive onto the periodic orbit. It is produced in the same manner as the unstable manifold, but integrating time backwards instead of forward. See Howell et al.[13] or Parker and Chua[14] for more details regarding the construction of these manifolds.

## II. Simple-Periodic Symmetrical Orbits

Several families of simple-periodic symmetrical orbits have been found in the Earth-Moon system. Matukuma[15,16] and Strömgren[1] classified five families of such orbits using the nomenclatures shown in Table 1, based on where the families originated.

**Table 1. Classification of symmetric periodic orbits in the PCRTBP based on their origins.**

| Author | Origin of the Family $L_2$ | $L_1$ | $M_2$ Retrograde | $M_2$ Prograde | Branch of $g$ |
|---|---|---|---|---|---|
| Matukuma | $F$ | $F$ | $a$ | $A, B$ | $H, E, I_2, G$ |
| Strömgren | $a$ | $c$ | $f$ | $g$ | $g'$ |

The trouble with the classic scheme for classifying symmetric periodic orbit families is that the family gradually moves around the system until it may not be clear which object is at its center. In this study the orbits of interest are still in portions of their respective families that are near their origin, thus this classification scheme would work well. However, the interest is to pursue more complicated trajectories in the future and therefore another classification scheme is preferable. Broucke[17] conjectured that since this type of orbit pierces the $x$-axis two times orthogonally, one could introduce six classes that would easily contain all such periodic orbits based on the locations of those piercings. The "center" of the orbit would then be clearly defined. Furthermore, one family of orbits is always contained within a single class. The classes and a pictorial description are listed in Table 2.

**Table 2. Classification of symmetric periodic orbits in the PCRTBP based on their orthogonal $x$-axis crossings.**

| Class | Structure | Center |
|---|---|---|
| Class 1 | $x_0$ — $x_1$ — $M_1$ — $M_2$ → | $L_3$ |
| Class 2 | $x_0$ — $M_1$ — $x_1$ — $M_2$ → | $M_1$ |
| Class 3 | $x_0$ — $M_1$ — $M_2$ — $x_1$ → | $M_1$+$M_2$ |
| Class 4 | $M_1$ — $x_0$ — $x_1$ — $M_2$ → | $L_1$ |
| Class 5 | $M_1$ — $x_0$ — $M_2$ — $x_1$ → | $M_2$ |
| Class 6 | $M_1$ — $M_2$ — $x_0$ — $x_1$ → | $L_2$ |

The initial conditions of the simple-periodic symmetrical orbits found in the Earth-Moon system that did not hit the earth's surface or the moon's surface are shown in Figures 4 and 5, below. Figure 4 shows those orbits whose initial conditions lay on the far side of the moon, between the moon and $LL_2$; Figure 5 shows the orbits with initial conditions between the earth and moon. In both cases the gray orbits are neutrally stable and the black orbits are unstable. Special attention was paid in search of orbits near the moon; hence several families of periodic orbits are certainly missing whose initial conditions lie on the opposite side of the earth. Those will be explored in a later paper.

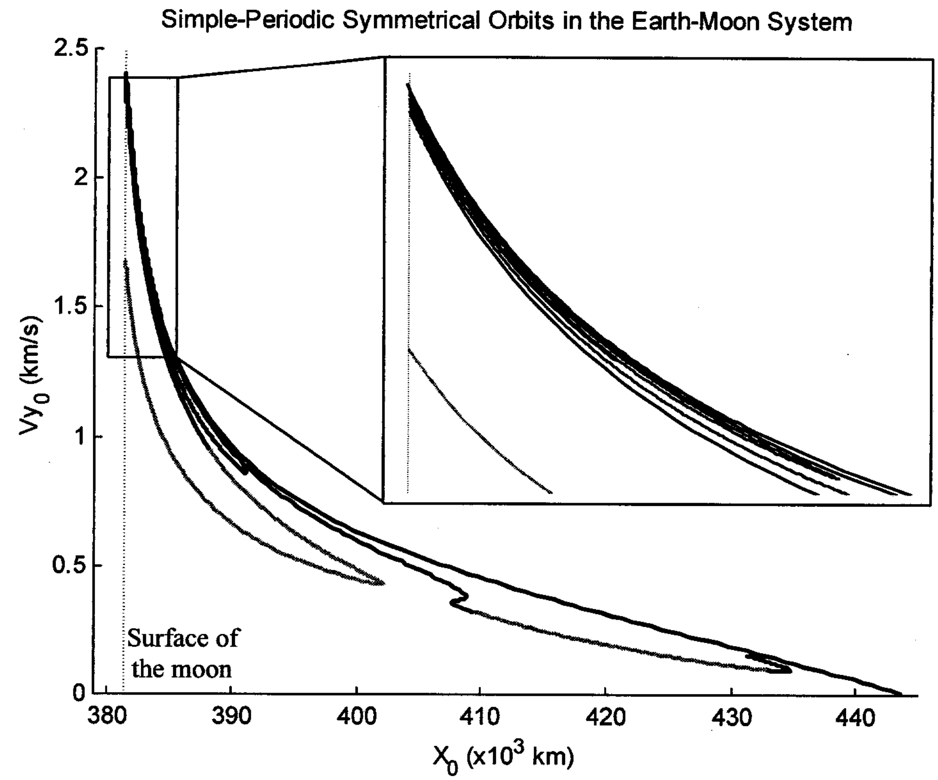


**Figure 4. The initial conditions of simple-periodic symmetrical orbits in the Earth-Moon system. The orbits in gray are neutrally stable; the orbits in black are unstable.**

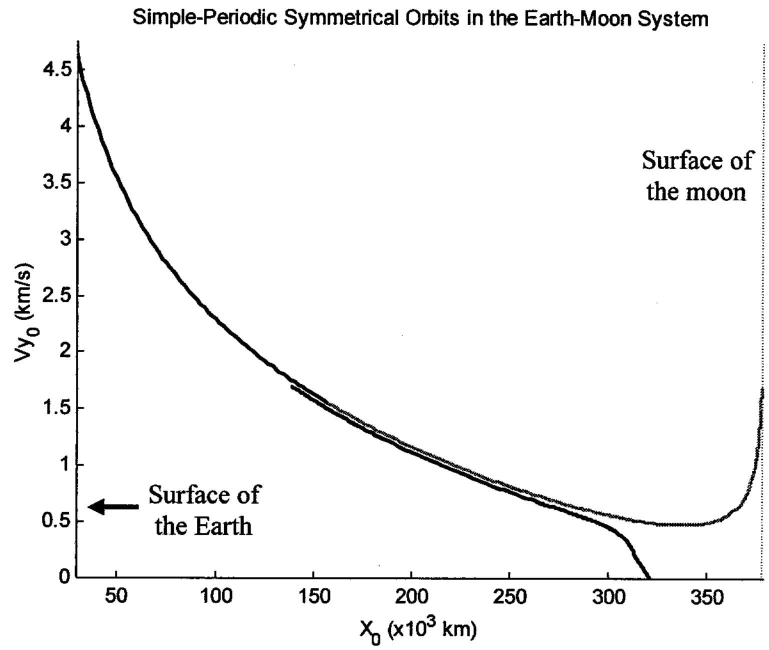


**Figure 5. The initial conditions of simple-periodic symmetrical orbits on the near side of the moon in the Earth-Moon system. The orbits in gray are neutrally stable; the orbits in black are unstable.**

Figure 6 shows the periodic orbits' Jacobi constant as functions of $x_0$ for those orbits given in Figure 4. The orbit families are labeled corresponding to the classification scheme given in Table 2 with Strömgren's classification from Table 1 in parentheses; the bold-letter families are arbitrary family identifiers used in this paper. Brief descriptions of these lettered families are given in Table 3, below.

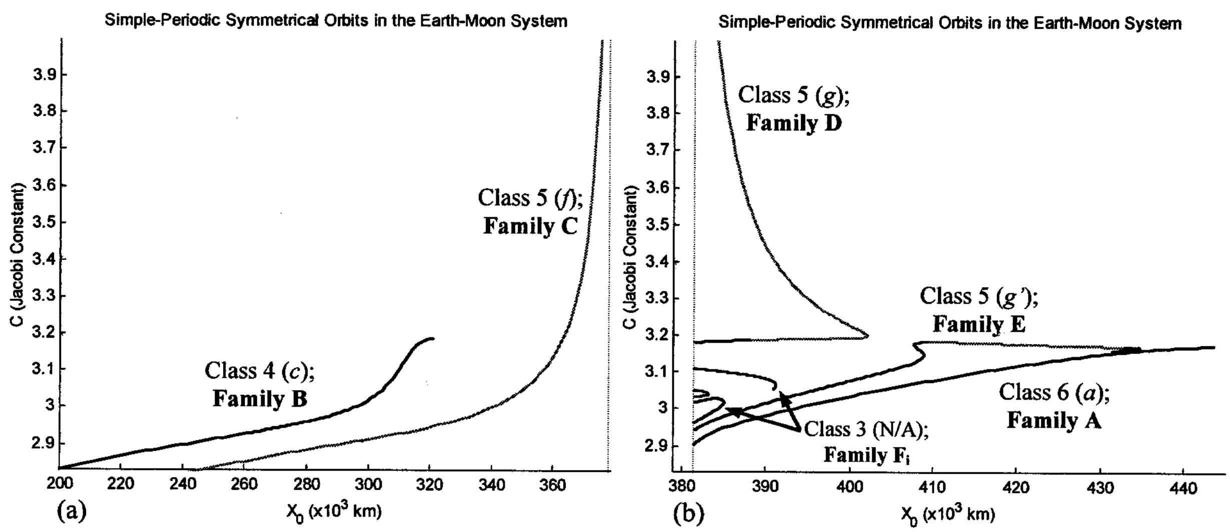


**Figure 6. The periodic orbits' Jacobi constant as functions of $x_0$ for periodic orbits whose initial conditions are on the left (a) and right (b) side of the moon. The labels are classifications based on Table 2 with Strömgren's classification in parentheses. The bold letter labels are arbitrary and only used to identify the different curves in this study.**

Table 3. A brief description of each of the families presented in this study.

| Family | Broucke's Classification | Description |
|---|---|---|
| A | Class 6 | Lyapunov orbits about $LL_2$. |
| B | Class 4 | Lyapunov orbits about $LL_1$. |
| C | Class 5 | Distant retrograde orbits about the moon. |
| D | Class 5 | Low prograde orbits about the moon. |
| E | Class 5 | Distant prograde orbits about the moon. |
| $F_i$ | Class 3 | Periodic resonant lunar flyby orbits. |

Figure 7 shows the periods of the orbits as functions of $x_0$ for those orbits given in Figure 4. The orbit families are labeled corresponding to the classification scheme given in Table 2 with Strömgren's classification from Table 1 in parentheses. The bold-letter families are arbitrary family identifiers used in this paper.

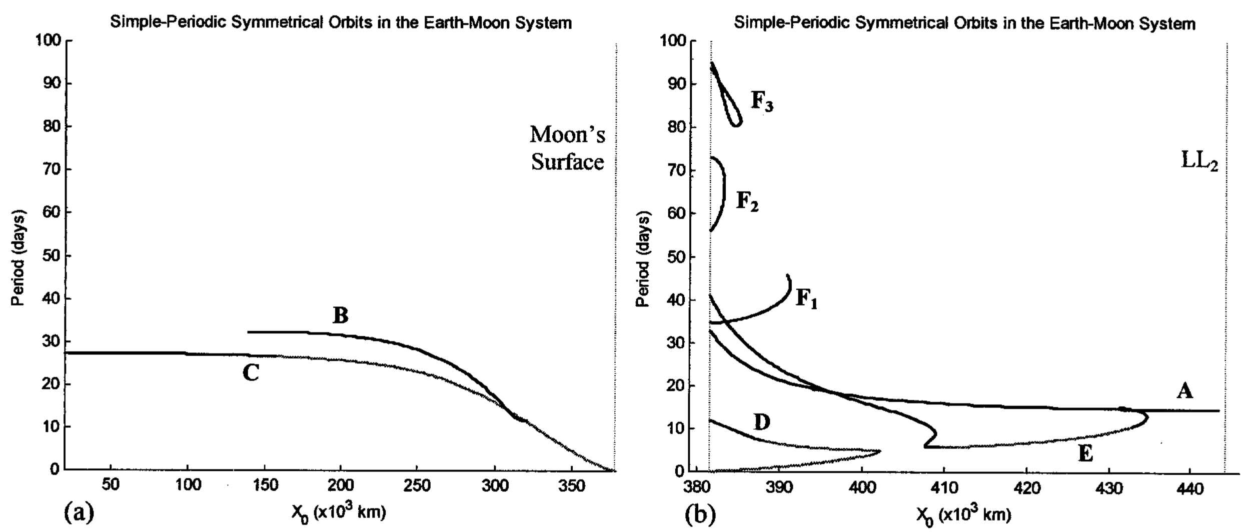


**Figure 7. The periods of the orbits as functions of $x_0$ for periodic orbits whose initial conditions are on the left (a) and right (b) side of the moon. The bold letter labels correspond with the families of the same identifier in Figure 6.**

The orbits in each of the families will now be examined in more detail.

## A. Family A: Lyapunov orbits about $LL_2$

Family A was chosen to begin this examination since it was used as the example in Figures 2 and 3. This family of periodic orbits is commonly known as the family of Lyapunov orbits about the lunar $L_2$ point. Figure 8 shows the full state space curve of initial conditions that produce these orbits, up until they impact the lunar surface. Theoretically this family continues, but since this study is concerned with potential mission designs it will not dwell on families that extend into the lunar surface. Figure 9 shows characteristic Lyapunov orbits of this type in position and velocity space.

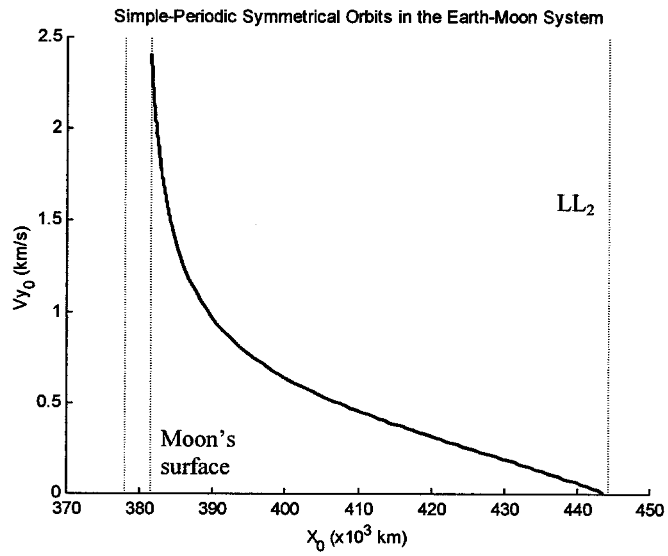


**Figure 8. The curve of initial conditions that produce Family A, the family of Lyapunov orbits about $LL_2$.**

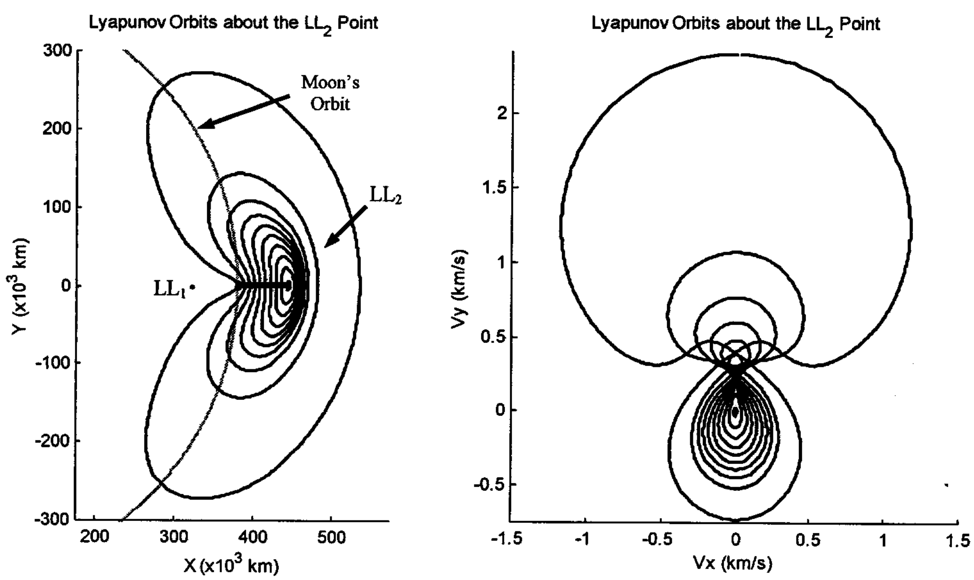


**Figure 9. The position (left) and velocity (right) plots of Family A: the family of Lyapunov orbits about $LL_2$.**

The stable and unstable invariant manifolds of two representative Lyapunov orbits are shown in Figures 10 and 11. The trajectories on the manifolds were propagated for approximately one month. The initial conditions and Jacobi constants for these orbits are given in Table 4.

**Table 4. The initial conditions and Jacobi constants for the Lyapunov orbits shown in Figures 10 and 11, given in normalized units.**

| Orbit | $x_0$ | $vy_0$ | $C$ |
|---|---|---|---|
| Figure 10 | 1.11862643 | 0.18438956 | 3.15035182 |
| Figure 11 | 1.02757544 | 0.74692043 | 3.00995185 |

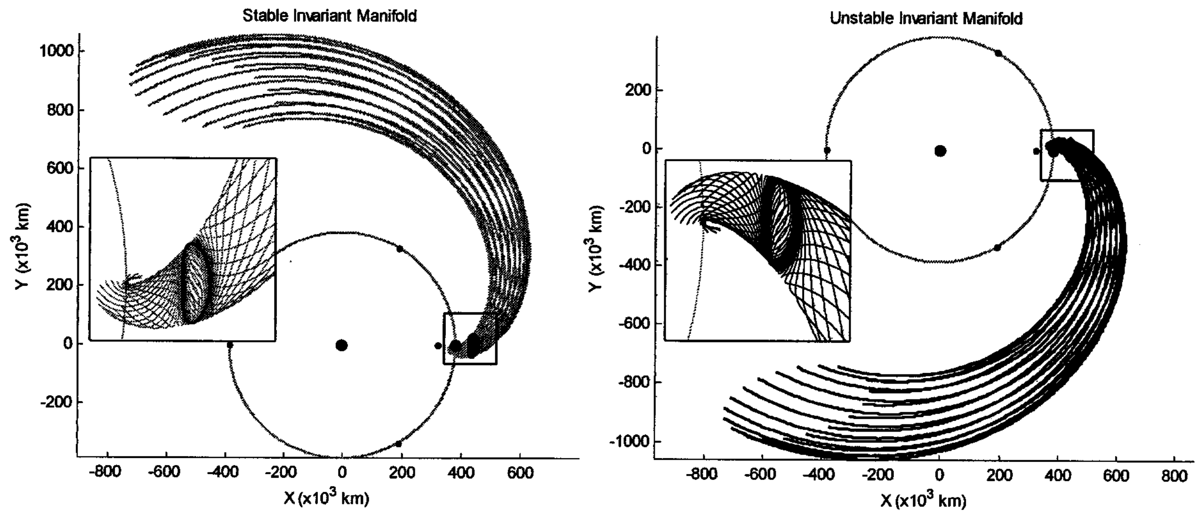


**Figure 11. The stable (left) and unstable (right) invariant manifolds of a Lyapunov orbit about $LL_2$ that has a Jacobi constant of 3.15035182.**

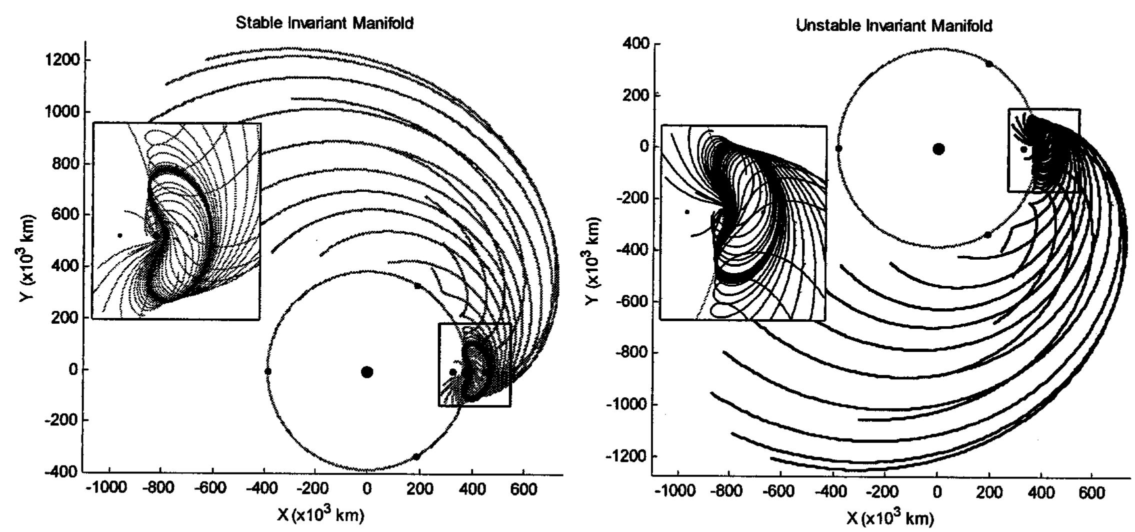


**Figure 10. The stable (left) and unstable (right) invariant manifolds of a Lyapunov orbit about $LL_2$ that has a Jacobi constant of 3.00995185.**

### B. Family B: Lyapunov orbits about $LL_1$

Family B of simple-periodic symmetrical orbits is much like Family A. It is commonly known as the family of Lyapunov orbits about the lunar $L_1$ point. Figure 12 shows the full state space curve of initial conditions that produce these orbits, up until they impact the lunar surface. Every orbit on the curve is asymptotically unstable. Figure 13 shows characteristic Lyapunov orbits of this type in position and velocity space.

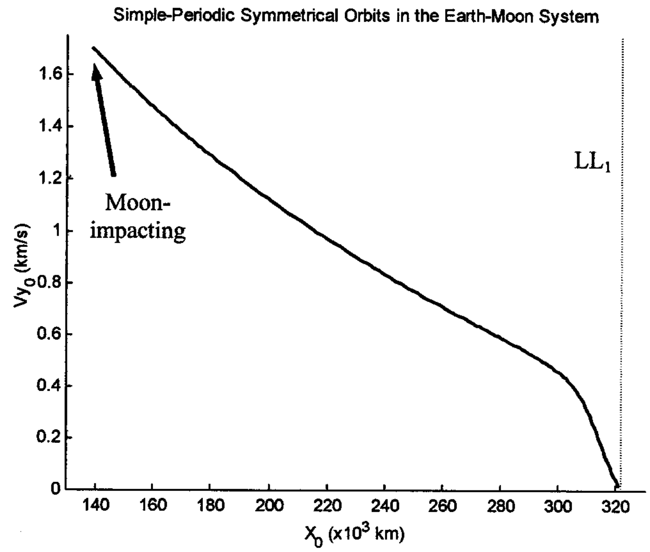


**Figure 12. The curve of initial conditions that produce Family B, the family of Lyapunov orbits about $LL_1$.**

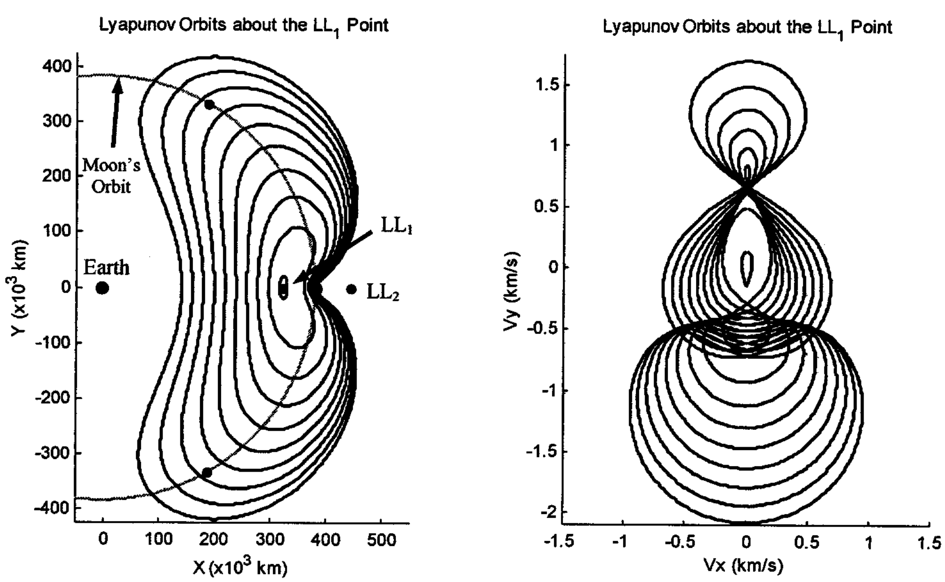


**Figure 13. The position (left) and velocity (right) plots of Family B: the family of Lyapunov orbits about $LL_1$.**

The stable and unstable invariant manifolds of two representative Lyapunov orbits are shown in Figures 14 and 15. The trajectories on the manifolds were propagated for approximately one month. The initial conditions and Jacobi constants for these orbits are given in Table 5.

**Table 5. The initial conditions and Jacobi constants for the Lyapunov orbits shown in Figures 14 and 15, given in normalized units.**

| Orbit | $x_0$ | $vy_0$ | $C$ |
|---|---|---|---|
| Figure 14 | 0.81165453 | 0.25479879 | 3.13004286 |
| Figure 15 | 0.71540062 | 0.60461823 | 2.95097632 |

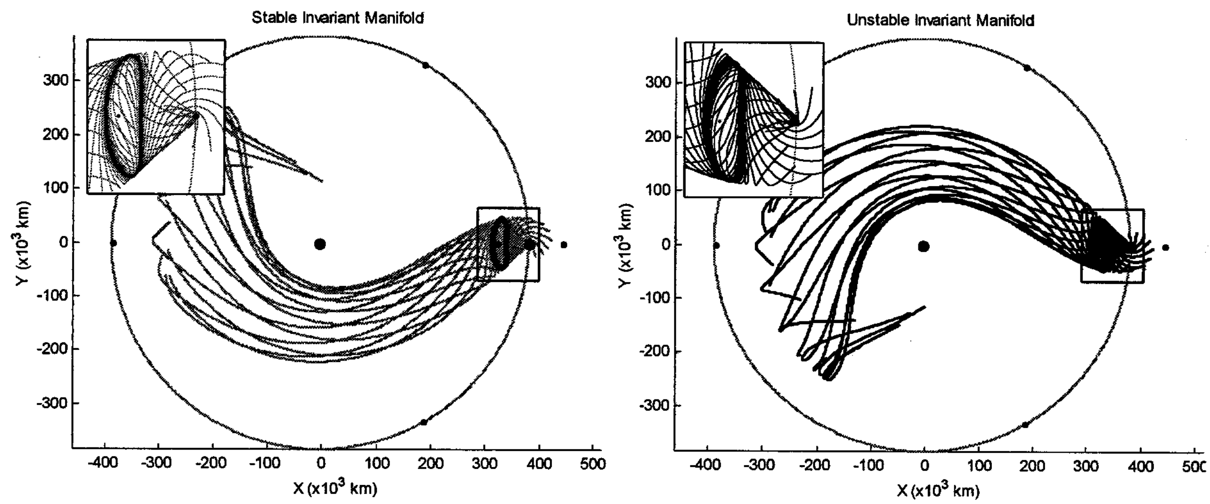


**Figure 14. The stable (left) and unstable (right) invariant manifolds of a Lyapunov orbit about $LL_1$ that has a Jacobi constant of 3.13004286.**

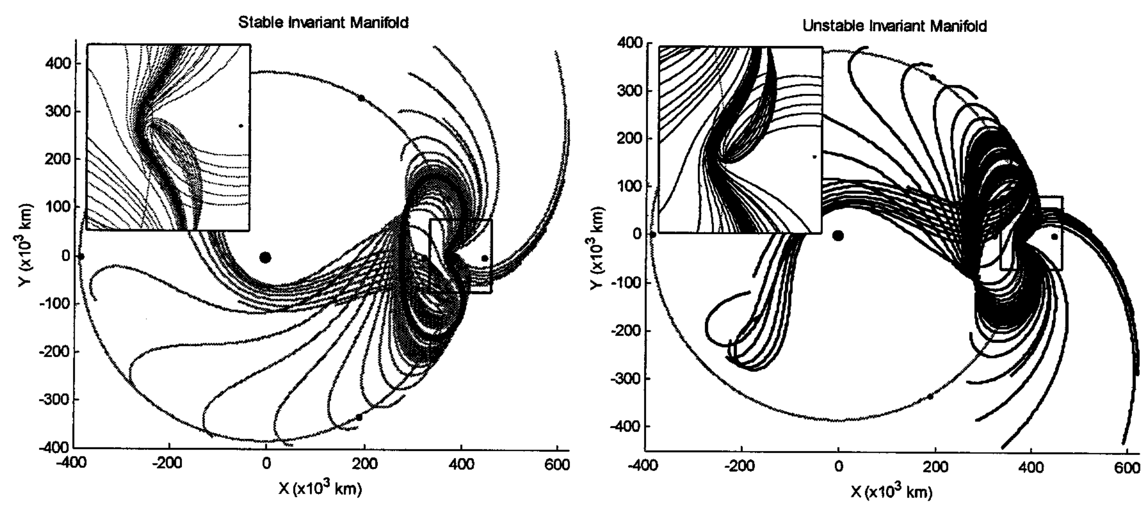


**Figure 15. The stable (left) and unstable (right) invariant manifolds of a Lyapunov orbit about $LL_1$ that has a Jacobi constant of 2.95097632.**

## C. Family C: Distant Retrograde Orbits (DROs) about the moon

Family C consists of orbits that traverse the moon in a retrograde fashion in the rotating frame. The family includes unstable and neutrally stable orbits, where the unstable orbits pass near the earth. Figure 16 shows the state space curve of initial conditions that produce these orbits, up until they impact either the earth's or the moon's surface. The gray portion of the curve indicates where the orbits are neutrally stable; the rest of the curve corresponds with unstable orbits. Figure 17 shows characteristic DROs of this type in position and velocity space.

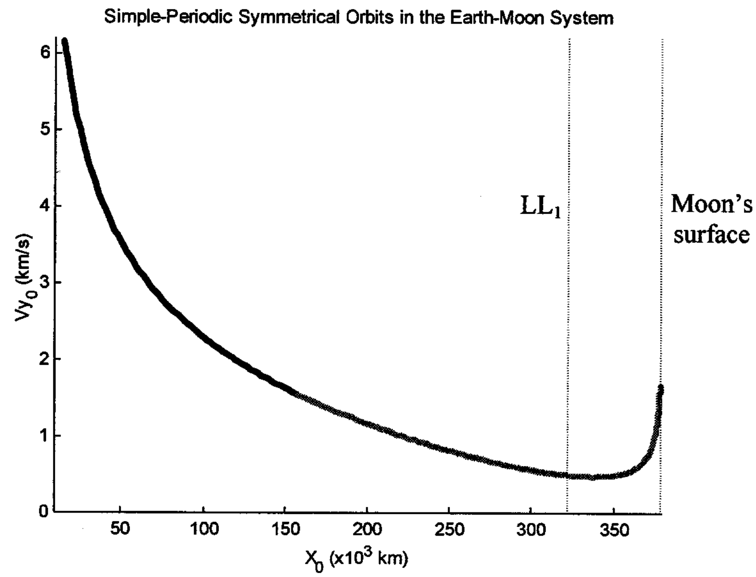


**Figure 16. The curve of initial conditions that produce Family C, the family of distant retrograde orbits about the moon. The points in gray represent neutrally stable orbits; the points in black represent unstable orbits.**

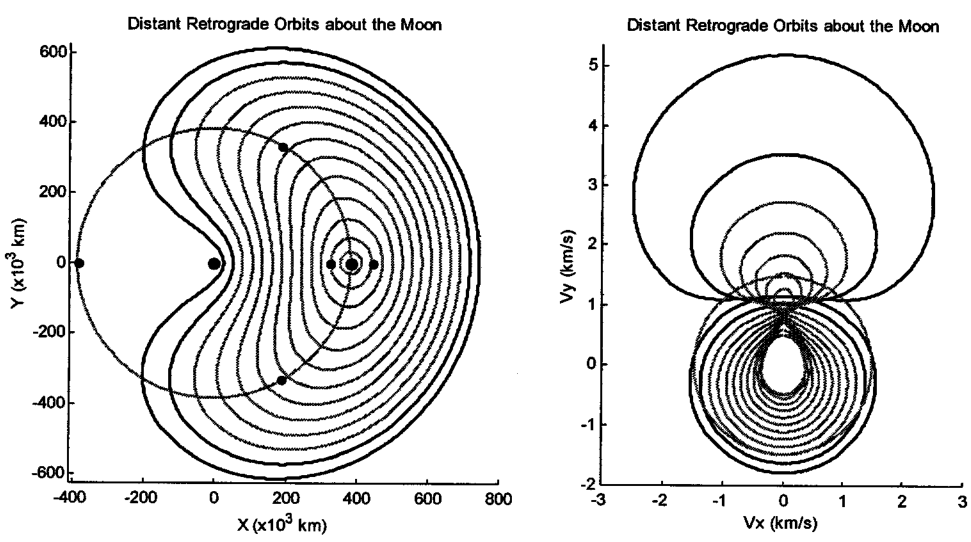


**Figure 17. The position (left) and velocity (right) plots of Family C: the family of distant retrograde orbits about the moon. The orbits in gray are neutrally stable; the orbits in black are unstable.**

The invariant manifolds of the DROs found in this study are generally not very interesting. The neutrally stable DROs, although great for station-keeping requirements, do not lend themselves to free transfers of any sort. The orbits that approach the earth, however, do experience brief moments of large instabilities as they pass by the earth. Figure 18 shows an example of a stable and an unstable invariant manifold produced from one of these unstable DROs. Only four trajectories were propagated on these manifolds, but those were propagated for a year. One can see that the earth's perturbations influence the trajectories to go nearly anywhere in the system, but the flow near the manifolds is stable except near the earth or moon. Table 6 lists the initial conditions and Jacobi constant for the host DRO.

**Table 6. The initial conditions and Jacobi constant for the DRO shown in Figure 18, given in normalized units.**

| Orbit | $x_0$ | $vy_0$ | $C$ |
|---|---|---|---|
| Figure 18 | 0.05202914 | 5.39508005 | 1.70562520 |

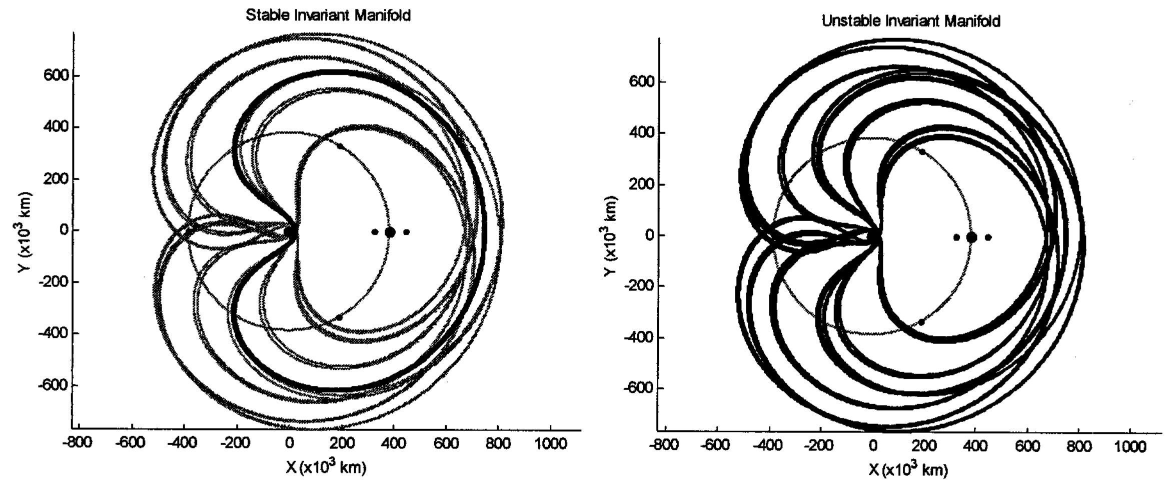


**Figure 18. The stable (left) and unstable (right) invariant manifolds for a distant retrograde orbit about the moon.**

### D. Family D: Low Prograde Orbits about the Moon

Family D consists of orbits that traverse the moon in a direct fashion in the rotating frame. The family includes unstable and neutrally stable orbits, where the unstable orbits pass near $LL_1$. Figure 19 shows the state space curve of initial conditions that produce these orbits, up until they impact the moon's surface. The gray portion of the curve indicates where the orbits are neutrally stable; the rest of the curve corresponds with unstable orbits. Figure 20 shows characteristic low prograde orbits of this type in position and velocity space.

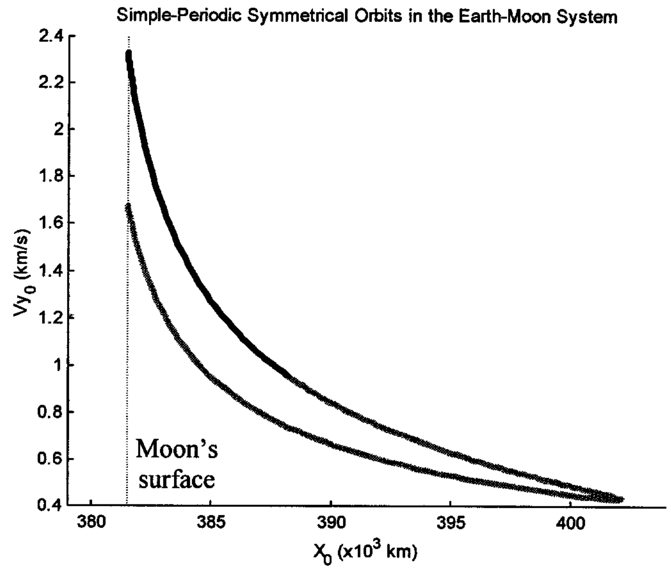


**Figure 19. The curve of initial conditions that produce Family D, the family of low prograde orbits about the moon. The points in gray represent neutrally stable orbits; the points in black represent unstable orbits.**

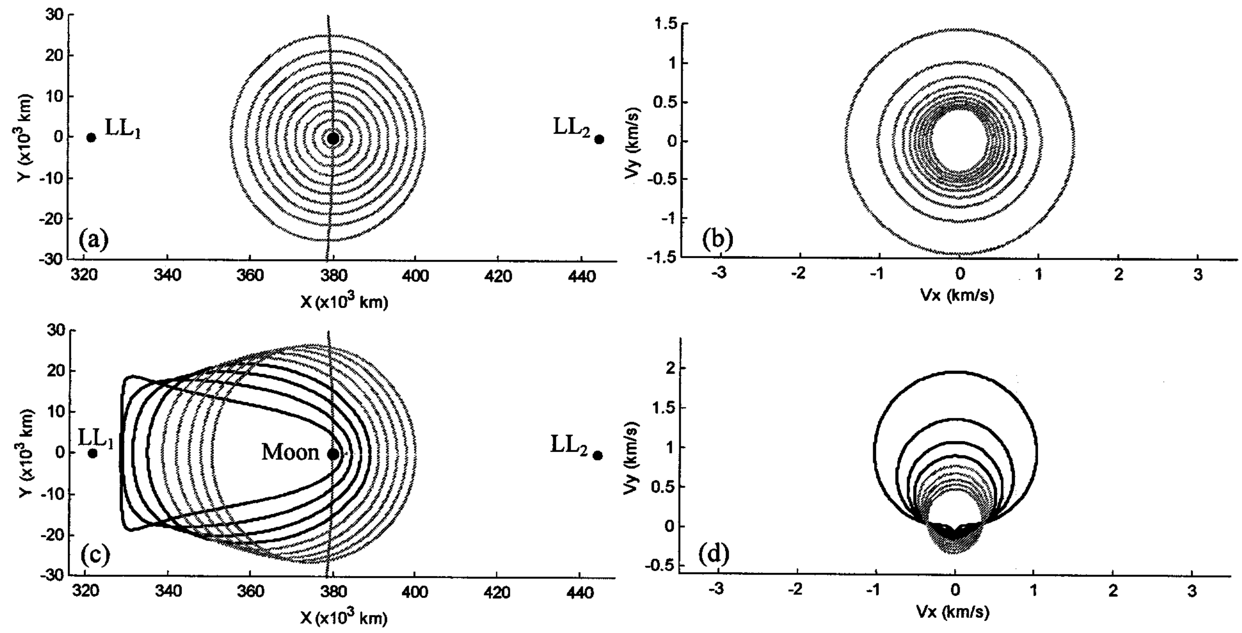


**Figure 20. State space plots of Family D: the family of low prograde orbits about the moon. Position plots are continued in (a) and (c); velocity plots are continued in (b) and (d). The orbits in gray are neutrally stable; the orbits in black are unstable.**

The invariant manifolds of the family of low prograde orbits are interesting as the orbit family approaches $LL_1$. An example set of stable and unstable invariant manifolds of this family is shown in Figure 21. The trajectories in the manifold have been propagated for approximately two weeks. The structure in these manifolds is less pronounced than in the Lyapunov orbit manifolds, mostly due to the close proximity of these manifolds to the moon. The initial conditions and Jacobi constant for this orbit are shown in Table 7.

**Table 7. The initial conditions and Jacobi constant for the low prograde orbit shown in Figure 21, given in normalized units.**

| Orbit | $x_0$ | $vy_0$ | $C$ |
|---|---|---|---|
| Figure 21 | 0.99900000 | 1.39554029 | 3.18374229 |

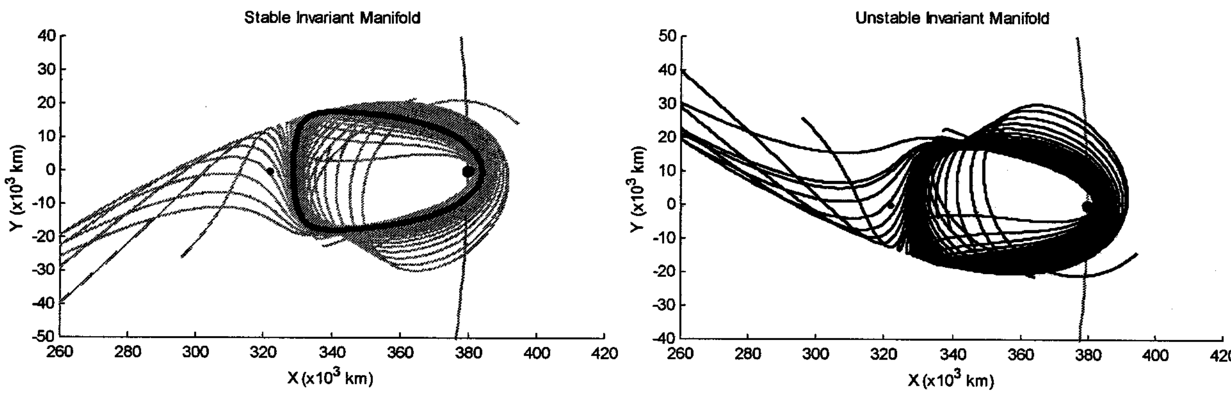


**Figure 21. The stable (left) and unstable (right) invariant manifolds of a low prograde orbit about the moon.**

## E. Family E: Distant Prograde Orbits about the Moon

Family E consists of some of the most interesting direct orbits about the moon. The family includes a neutrally stable region that would have branched from Family D in the case when $\mu = 0$. Continuing that region toward $LL_2$ one finds orbits that are nearly symmetrical to those found in Family D; continuing toward the moon's surface one finds orbits that loop around in the rotating frame, eventually making two close flybys of the moon per period. Figure 22 shows the state space curve of initial conditions that produce these orbits, up until they impact the moon's surface. Figure 23 shows characteristic distant prograde orbits of this type in position and velocity space.

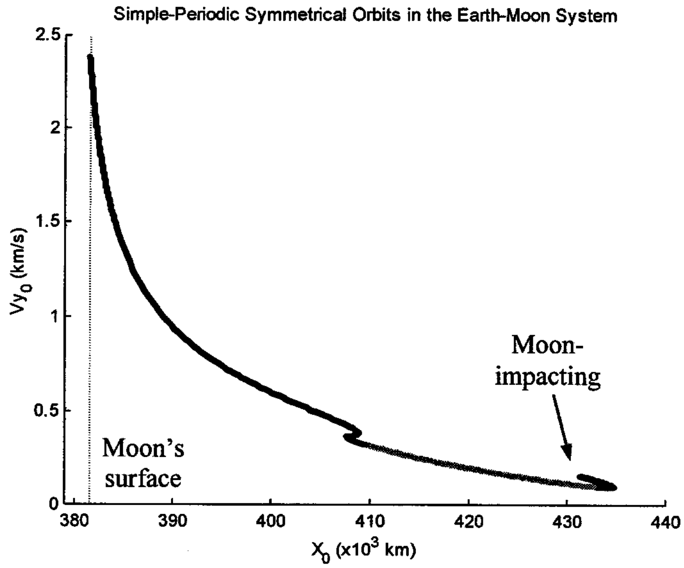


**Figure 22. The curve of initial conditions that produce Family E, the family of distant prograde orbits about the moon. The points in gray represent neutrally stable orbits; the points in black represent unstable orbits.**

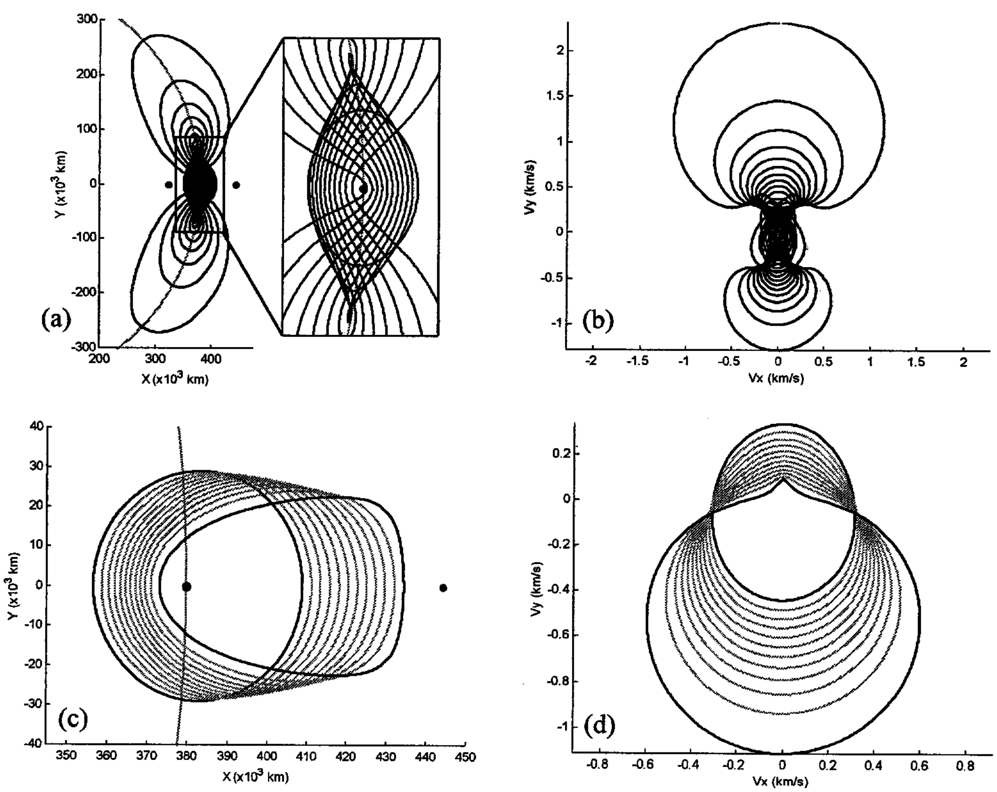


**Figure 23. State space plots of Family E: the family of distant prograde orbits about the moon. Position plots are continued in (a) and (c); velocity plots are continued in (b) and (d). The orbits in gray are neutrally stable; the orbits in black are unstable.**

The invariant manifolds of the family of distant prograde orbits are interesting as the orbit family approaches the moon. The invariant manifolds of the orbits that approach $LL_2$ are similar to those that approach $LL_1$ from Family D and won't be reproduced here. Figures 24 and 25 show two example sets of stable and unstable invariant manifolds of Family E. The trajectories in the manifold have been propagated for approximately one month. The structure in these manifolds includes sharp features as the trajectories approach the moon's surface. The initial conditions and Jacobi constant for this orbit are shown in Table 8.

**Table 8. The initial conditions and Jacobi constants for the distant prograde orbits shown in Figures 24 and 25, given in normalized units.**

| Orbit | $x_0$ | $vy_0$ | $C$ |
|---|---|---|---|
| Figure 24 | 1.05641000 | 0.45166031 | 3.11538832 |
| Figure 25 | 1.00936524 | 1.03951539 | 3.00176743 |

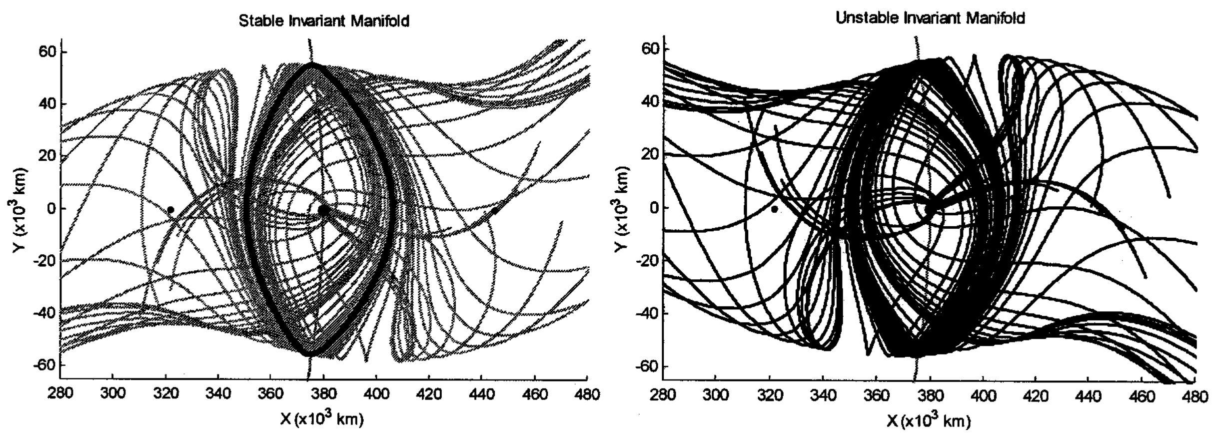


**Figure 25. The stable (left) and unstable (right) invariant manifolds of a distant prograde orbit about the moon. The Jacobi constant for this orbit is approximately equal to 3.11538832.**

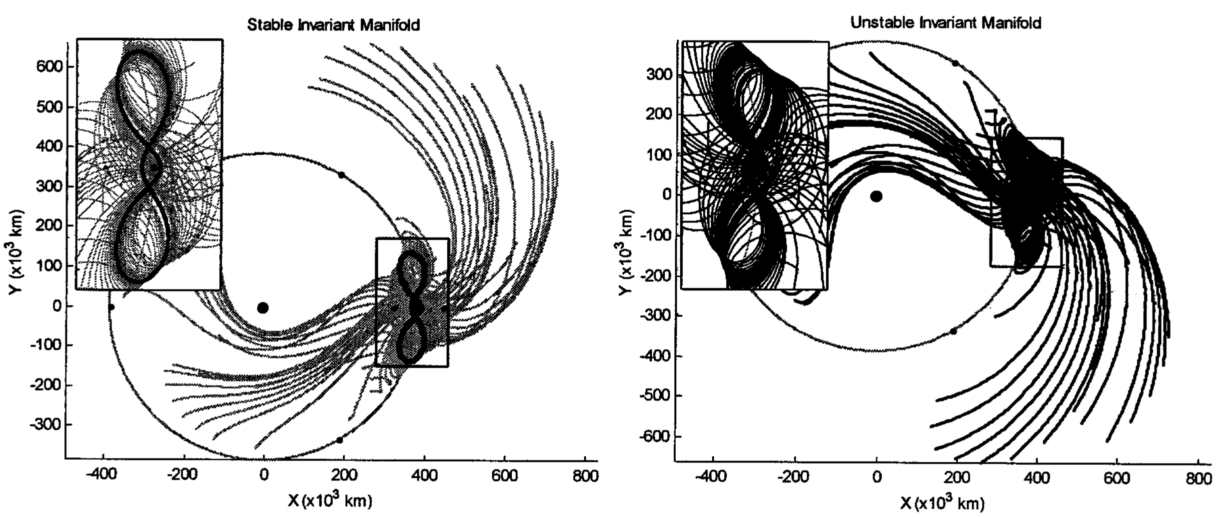


**Figure 24. The stable (left) and unstable (right) invariant manifolds of a distant prograde orbit about the moon. The Jacobi constant for this orbit is approximately equal to 3.00176743.**

## F. Family F: Periodic Resonant Lunar Flyby Orbits

Family F consists of orbits that make periodic close flybys of the moon while orbiting the earth in nearly two-body motion. These periodic flybys may occur at any resonance with the moon. This paper has explored three such families that fly by the moon beyond its radius, safe for all missions designed in the PCRTBP. Figure 26 shows the state space curve of initial conditions that produce these orbits, up until they impact the moon's surface. It is more useful to plot $x_0$ vs. the orbit's period for these families because then the resonances may be identified more readily. The families constructed here have resonances near 3:2, 5:2, and 3:1 with the moon. The curves each continue, but by continuing the curves one would introduce orbits that struck the moon. However, those orbits certainly are useful if one is interested in impacting the moon or understanding orbits that do impact the moon (or depart from the moon). This will be discussed more later. Figure 27 shows characteristic orbits of this resonant periodic type in position and velocity space.

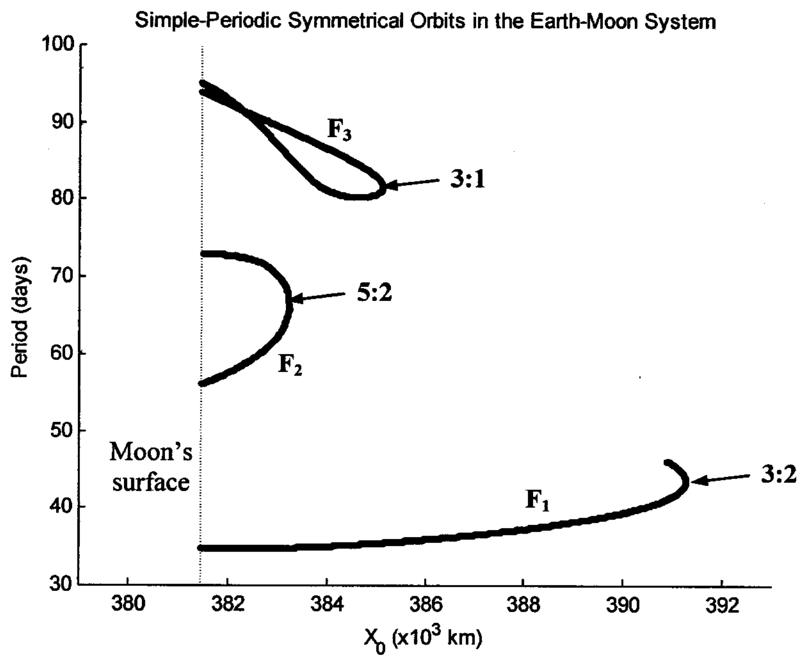


**Figure 26. The curve of initial conditions that produce Family F, the family of simple-periodic resonant flyby orbits. Every orbit shown here is unstable.**

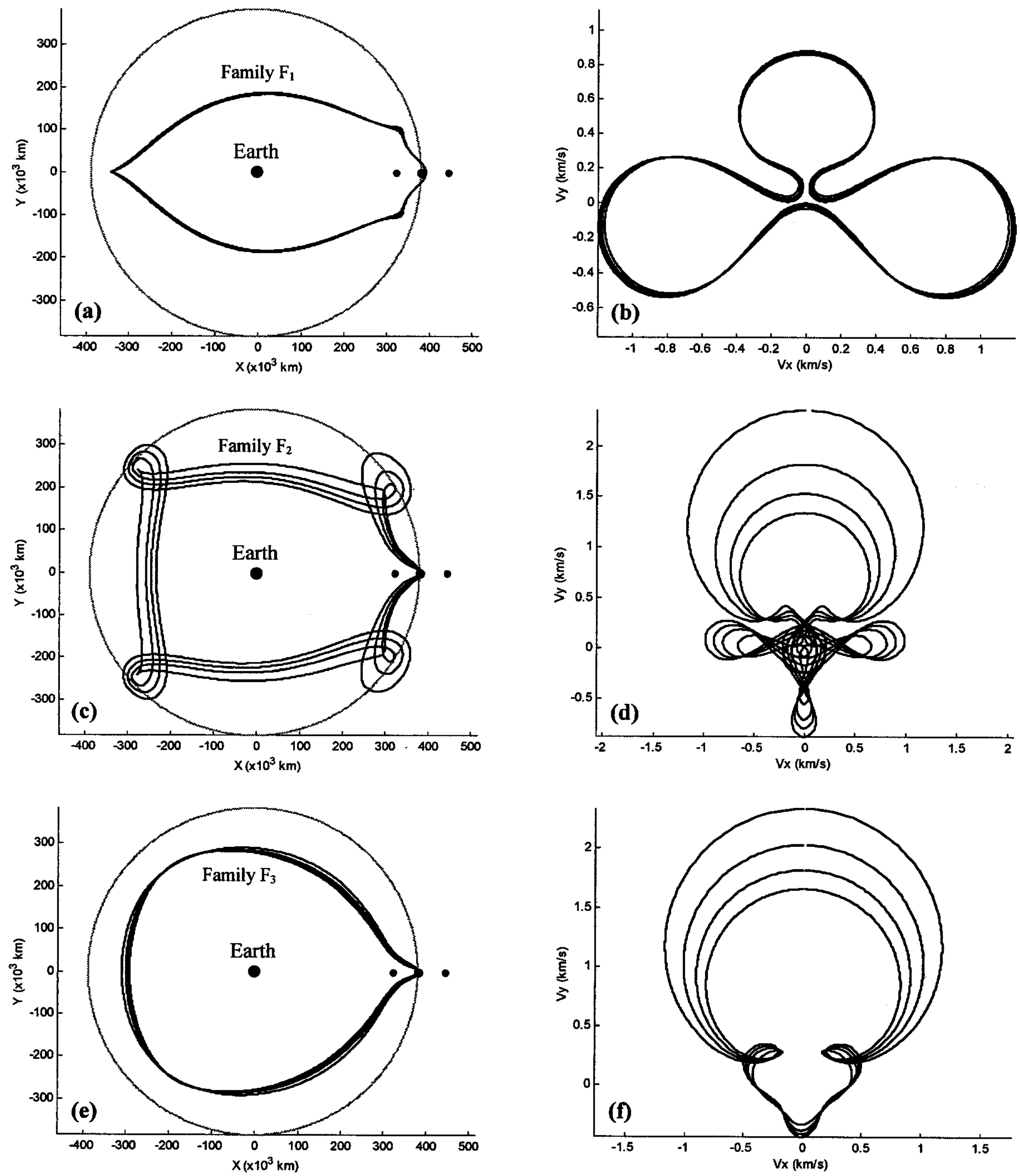


**Figure 27. State space plots of Family F: the family of distant resonant orbits about the moon. Family $F_1$ (3:2 resonance with the moon) is shown in (a) and (b); Family $F_2$ (5:2 resonance) is shown in (c) and (d); Family $F_3$ (3:1 resonance) is shown in (e) and (f). All of the orbits shown here are unstable.**

The invariant manifolds of the families of resonant flyby orbits are certainly interesting because of their close proximity to the moon. The dynamics are very stable during the lengthy trip around the earth since the moon's perturbation at those distances is minimal. Nonetheless, the small deviations about the nominal periodic orbit will be much more magnified as the third body draws nearer to the moon and during the lunar flybys. This characteristic of the orbit's stability is observable from the stable manifold plotted in Figure 28 (symmetric to the unstable manifold). This manifold corresponds to an example periodic orbit from the $F_1$ family. One can see in the blow-up of the region near the moon that the trajectories were bunched prior to the lunar swingby; the trajectories spread out much more noticeably after the encounter. The trajectories in the manifold were propagated for approximately six weeks. The initial conditions and Jacobi constant for this orbit are shown in Table 9.

**Table 9. The initial conditions and Jacobi constants for the distant prograde orbits shown in Figures 24 and 25, given in normalized units.**

| Orbit | $x_0$ | $vy_0$ | $C$ |
|---|---|---|---|
| Figure 28 | 1.01703000 | 0.85628297 | 3.05359715 |

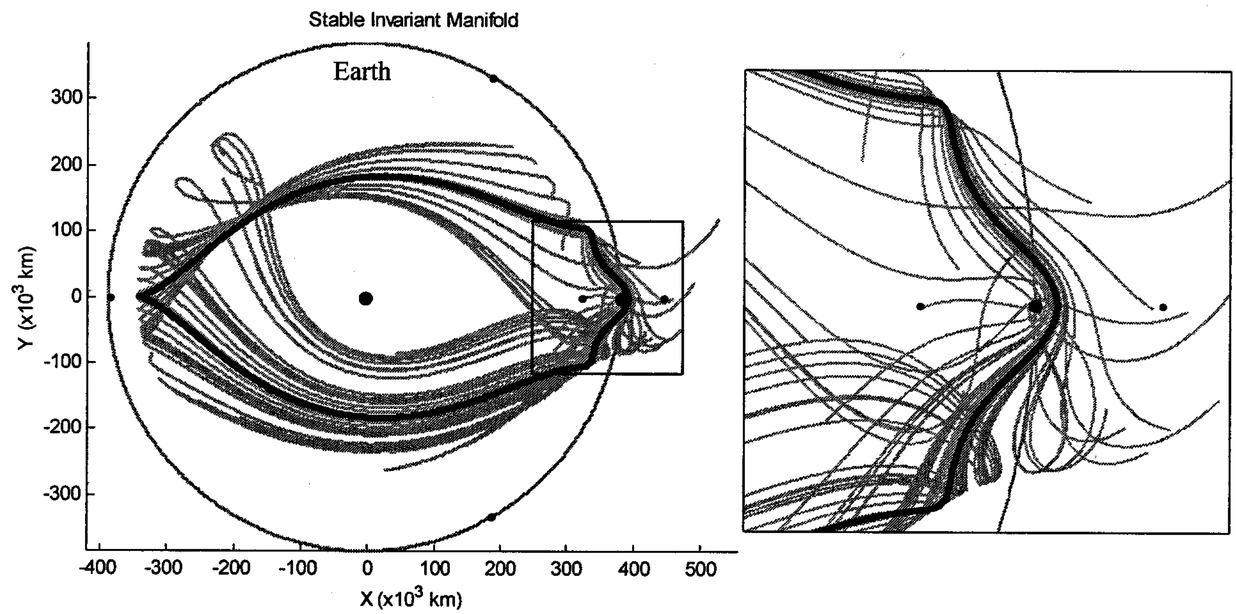


**Figure 28. The stable invariant manifold of a resonant lunar flyby orbit in the Earth-Moon system. Notice in the blow-up how the trajectories spread out after the flyby with the moon.**

## III. Orbit Transfers

Once a particle or spacecraft is on an unstable periodic orbit in the three-body system, then it may theoretically stay there for an arbitrarily long time or it may fall off of that orbit by following any trajectory on that orbit's unstable manifold. Theoretically the manifolds approach the unstable periodic orbits asymptotically and a particle on the orbit would take an infinite amount of time to depart; but in the real world there are constant perturbations and one is never actually on the periodic orbit. Thus the cost of controlling the departure in a real mission is the same order of magnitude as station-keeping.

One may notice by studying the unstable manifolds from the orbits given in the previous section that by controlling exactly when the spacecraft departs from its periodic orbit, it may be able to transfer to numerous other locations in the state space, including, but not limited to, the surface of the moon, any of the five lunar Lagrange points, another unstable periodic orbit in the system, or an escape trajectory away from the vicinity of Earth. The spacecraft may perform any of these transfers for free if the destination has the same Jacobi energy as the spacecraft's host periodic orbit. If not, then at least one maneuver will be required to change the spacecraft's Jacobi energy‡.

### A. Heteroclinic Transfers

A free transfer from one periodic orbit to another is known as a heteroclinic transfer. These transfers are theoretical constructs since the trajectories on an orbit's stable invariant manifold asymptotically approach the orbit without ever achieving the orbit. Nevertheless, heteroclinic transfers in the PCRTBP are a good approximation for free transfers in the real system. Figure 29 shows a plot of the orbit families given in this paper and their Jacobi constants. Any two unstable orbits with the same energy may have a free transfer between them. The regions outside of this plot are less interesting in terms of free orbit transfers because the orbits outside of this region are largely stable orbits.

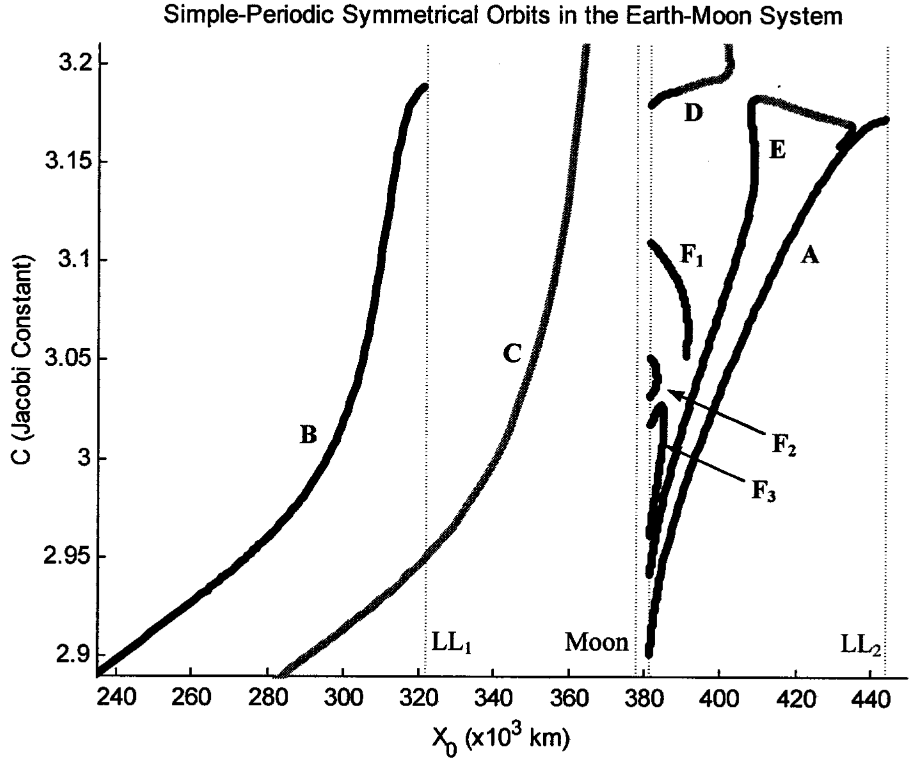


**Figure 29. A state space diagram of the periodic orbits in this paper. The black curves are unstable orbits; any two unstable orbits with the same Jacobi constant have a set of free transfers between them.**

To construct a free transfer between two unstable periodic orbits, one only needs to find the intersection of the first orbit's unstable manifold with the second orbit's stable manifold. At any intersection in position-space, the third body may perform a maneuver to transfer onto the new manifold, where the required $\Delta V$ is the difference in velocities between the two manifolds at the intersection. If the two manifolds intersect in position *and* velocity then the transfer is free. Free transfers require the third body to depart from its origin orbit at precisely the right time and then arrive onto the destination orbit at a specific point in the orbit. If those conditions are not ideal for a mission then a maneuver could be made to satisfy other mission criteria.

To demonstrate free transfers in the PCRTBP, this study has produced free transfers between unstable orbits in Families B and E (both B-E and E-B) and between unstable orbits in Families E and A for several different Jacobi energy values. Figures 30, 31, and 32 show these four transfers for Jacobi constants of 3.13443929, 3.09418559, and 2.96330290, respectively. Other transfers exist between Families D and B/E/A as well as between Families $F_i$ and B/E/A. Figure 33 shows the transfers between on orbit of Family $F_1$ with an orbit in Family A.

‡ This is true in the PCRTBP; however, in the real system the spacecraft or particle could have an interaction with another planetary body, solar radiation, drag, etc, that would alter its Jacobi energy.

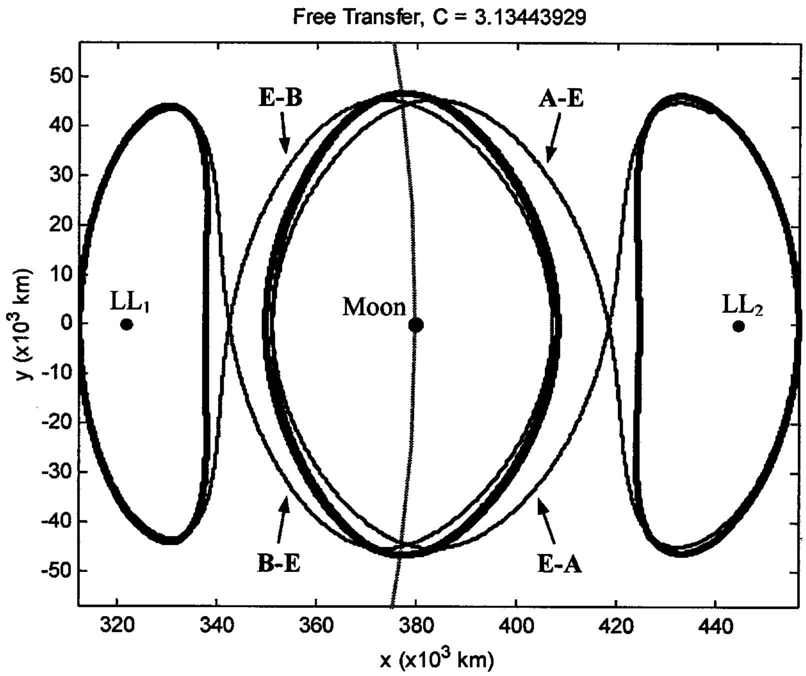


**Figure 30. Free transfers between Families B (Lyapunov orbits about $LL_1$), E (distant prograde orbits about the moon), and A (Lyapunov orbits about $LL_2$) where all three orbits have the same Jacobi constant C = 3.13443929.**

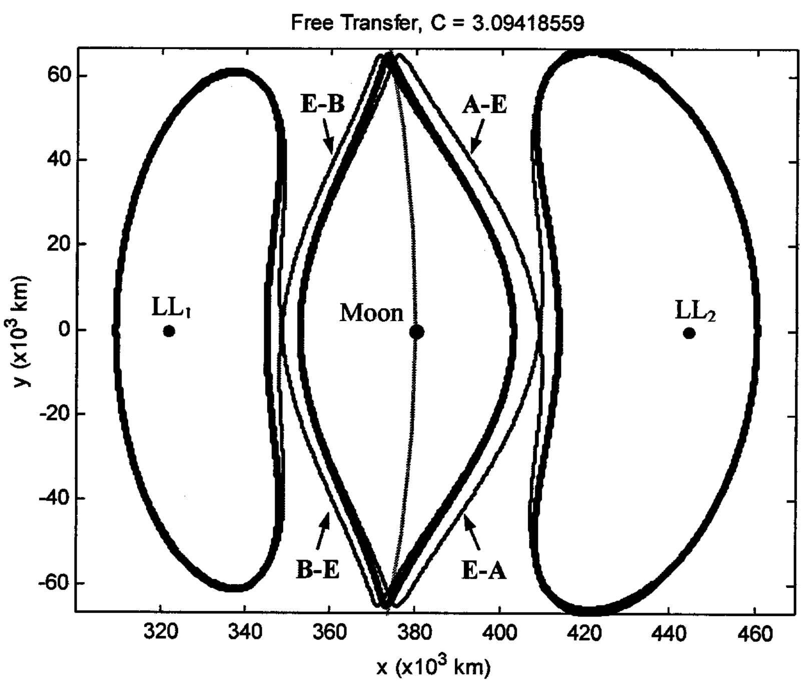


**Figure 31. Free transfers between Families B (Lyapunov orbits about $LL_1$), E (distant prograde orbits about the moon), and A (Lyapunov orbits about $LL_2$) where all three orbits have the same Jacobi constant C = 3.09418559.**

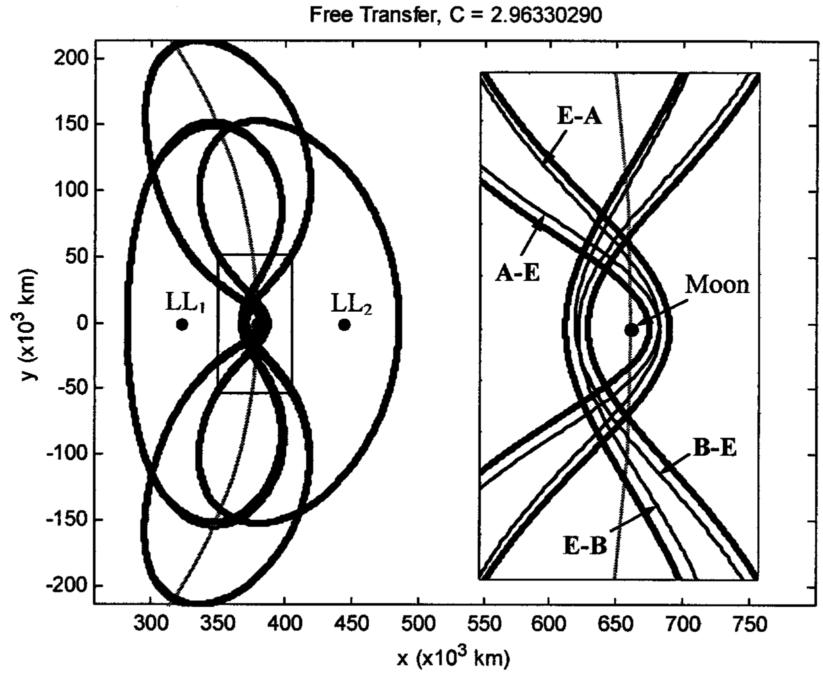


**Figure 32. Free transfers between Families B (Lyapunov orbits about $LL_1$), E (distant prograde orbits about the moon), and A (Lyapunov orbits about $LL_2$) where all three orbits have the same Jacobi constant C = 2.96330290.**

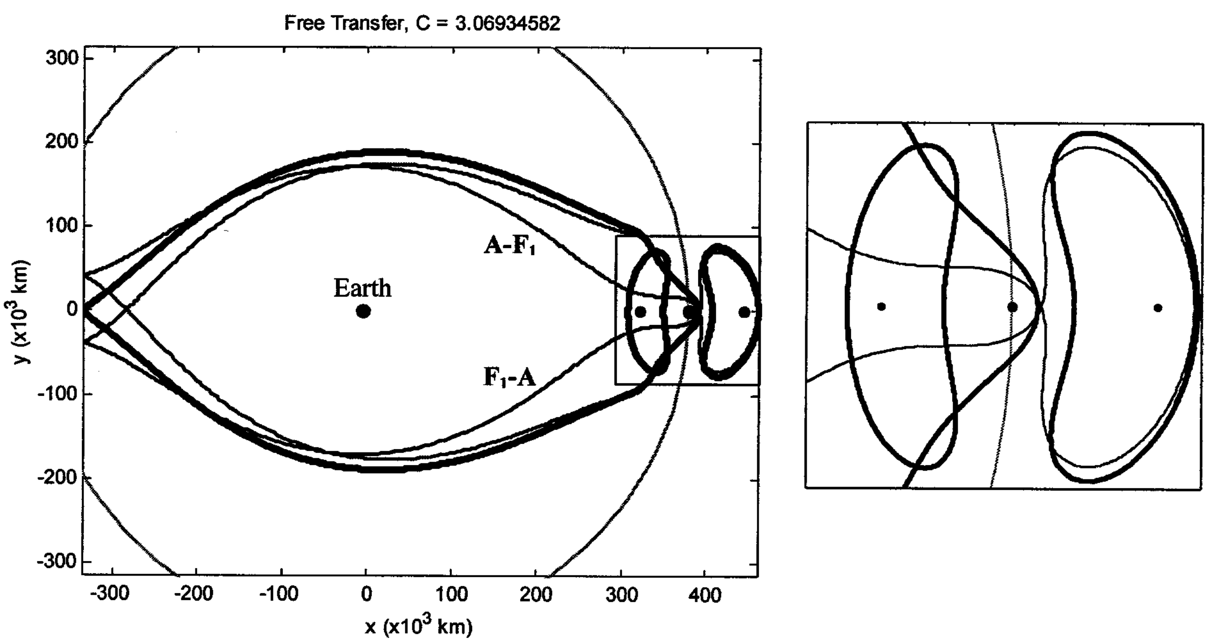


**Figure 33. Free transfers between an orbit in Family $F_1$ (Resonant lunar flyby orbit) and an orbit in Family A (Lyapunov orbits about $LL_2$) where both orbits have the same Jacobi constant C = 3.06934582.**

Since these orbit transfers are free, a combination of such transfers will constitute another periodic orbit solution in the PCRTBP. Several of these periodic transfers are introduced as periodic orbits in Ref. 18, e.g. orbits categorized in the Families *Hb* and $g_3$. In fact, due to the dynamics in the system, one may construct a trajectory that follows any unstable periodic orbit for $p_1$ periods, transfers to the vicinity of another periodic orbit and follows it for $p_2$ periods, transfers to another, *ad infinitum*, where the values of $p_i$, for $i = 1,2,\ldots,\infty$, are arbitrary non-negative integers[19]. If the sequence of $p_i$'s is periodic then one has constructed a periodic orbit solution in the PCRTBP. Thus, there are infinitely many periodic orbits in the system.

## IV. Mission Design Opportunities

It has been seen that one may transfer between unstable periodic orbits of equal energy for free. One may use this to construct a mission design architecture for the Earth-Moon three-body system, or for any other three-body system as well. This subject will be further discussed in later papers.

Many mission design options are available that may take advantage of the orbits shown in this paper. First of all, since there are heteroclinic connections between the various families of orbits, one always has the option to transfer to those other locations in the Earth-Moon space, provided that one has the correct energy level (and the required energy ranges are wide for the Lyapunov orbits and prograde orbits). If one is interested in escaping from the Earth-Moon system, one need only follow the unstable manifold of one of these unstable orbits. The orbits that pass very close to the moon, i.e., the large resonant orbits, have a wide range of possible escape trajectories since deviations near the moon are magnified greater than deviations away from the moon. The moon's influence may be used as a gravity slingshot to send spacecraft out on missions, but it may also be used as a target for returning spacecraft. An incoming spacecraft may target the stable manifold of an orbit that passes near the moon, such as a large, periodic resonant orbit. Then it may use that periodic orbit as a staging or quarantine orbit. The large resonant orbits are particularly interesting to be used as a quarantine or staging orbit because they require little station-keeping except when approaching and near the moon. Since there are so many resonant orbits, one may select the period of choice to be used as the staging orbit. From that orbit, the spacecraft could transfer for free to the surface of the moon, to other periodic orbits, such as the Lyapunov orbits, or to a trajectory that will fly by (or collide with) the earth.

## V. Conclusions

The exploration of simple periodic orbits in the PCRTBP has revealed that numerous orbits contain invariant manifolds that can be used in the Interplanetary Superhighway. It has been found that heteroclinic orbits exist between two unstable orbits in the PCRTBP that have the same Jacobi energy. The orbits' invariant manifolds provide a good way to locate these heteroclinic orbits quickly. Finally, these orbits provide a good foundation to be used when constructing an architecture for mission design options in the three-body problem. Additional work will be completed shortly extending the focus of this paper into the third dimension and outside of periodic symmetrical orbits. The extensions to this work appear promising for future mission design opportunities.

## Acknowledgments

This work has been completed under partial funding by by the National Aeronautics and Space Administration through Jet Propulsion Laboratory, California Institute of Technology; and by a National Defense Science and Engineering Graduate (NDSEG) Fellowship sponsored by the Deputy Under Secretary of Defense for Science and Technology and the Office of Naval Research.

We wish to express sincere gratitude for Dr. George Born, the director of the Colorado Center for Astrodynamics Research, who has supported us during this research.

## References

[1]Strömgren, E., "Connaissance actuelle des orbites dans le problème des trios corps," *Copenhagen Observatory Publications* No. 100; also *Bull. Astr.* Vol. 9, No. 87, 1935.

[2]Moulton, F.R., "Periodic Orbits," *Carnegie Institute of Washington Publications*, No. 161, 1920.

[3]Darwin, G.H., "Periodic Orbits," *Scientific Papers*, Vol. 4, Cambridge University Press, Cambridge, Mass., 1911.

[4]Hénon, M., "Exploration Numérique du Problème des Trois Corps, (I), Masses Egales, Orbites Périodiques," *Ann. Astrophys.*, Vol. 28, No. 3, pp. 499-511, 1965.

[5]Hénon, M., "Exploration Numérique du Problème des Trois Corps, (II), Masses Egales, Orbites Périodiques," *Ann. Astrophys.*, Vol. 28, No. 6, pp. 992-1007, 1965.

[6]Hénon, M., "Exploration Numérique du Problème des Trois Corps, (III), Masses Egales, Orbites Non Périodiques," *Bull. Astron.*, Vol. 1, No. 1, pp. 57-80, 1966.

[7]Hénon, M., "Exploration Numérique du Problème des Trois Corps, (IV), Masses Egales, Orbites Non Périodiques," *Bull. Astron.*, Vol. 1, No. 2, pp. 49-66, 1966.

[8]Hénon, M., "Numerical Exploration of the Restricted Problem. V., Hill's Case: Periodic Orbits and Their Stability," *Astron. & Astrophys.*, 1, 223-238, 1969.

[9]Koon, W.S., Lo, M.W., Marsden, J.E., & Ross, S.D., "Shoot the Moon," *Spaceflight Mechanics 2000*, AAS, Vol. 105, Part II, 1017-1030, 2000.

[10]Vallado, D.A., *Fundamentals of Astrodynamics and Applications*, McGraw-Hill Companies, Inc., 1997.

[11]Howell, K.C., "Three-Dimensional, Periodic, 'Halo' Orbits," *Celes. Mech.*, Vol. 32, No. 53, 1984.

[12]Strogatz, S.H., *Nonlinear Dynamics and Chaos*, Perseus Books Publishing, L.L.C., 1994.

[13]Howell, K.C., Barden, B.T., & Lo, M.W., "Application of Dynamical Systems Theory to Trajectory Design for a Libration Point Mission," *Journal of Astronautical Sciences*, Vol. 45, No. 2, pp. 161-178, April-June 1997.

[14]Parker, T.S. and Chua, L.O., *Practical Numerical Algorithms for Chaotic Systems*, Springer-Verlag, New York, 1989.

[15]Matukuma, T., *Proc. Imp. Acad. Japan*, Vol. 9, No. 364, 1933.

[16]Matukuma, T., *Sendai astr. Rap.*, No. 51, 1957.

[17]Broucke, R.A., "Periodic Orbits in the Restricted Three-Body Problem with Earth-Moon Masses," Technical Report 32-1168, Jet Propulsion Laboratory, Cal. Tech., 1968.

[18]Hénon, M., "New Families of Periodic Orbits in Hill's Problem of Three Bodies," *Celestial Mech. & Dynamical. Astr.*, Vol. 85, pp. 223-246, 2003.

[19]Koon, W.S., Lo, M.W., Marsden, J.E., & Ross, S.D., "Heteroclinic Connections Between Periodic Orbits and Resonance Transitions in Celestial Mechanics," *Chaos*, Vol. 10, No. 2, pp. 427-469, 2000.